*J. Fluid Mech.* (2007), *vol.* 584, *pp.* 203–223.  
doi:10.1017/S0022112007006404 Printed in the United Kingdom

# Two-layer quasi-geostrophic singular vortices embedded in a regular flow. Part 2. Steady and unsteady drift of individual vortices on a beta-plane

GREGORY REZNIK[1] AND ZIV KIZNER[2]†

[1]P. P. Shirshov Institute of Oceanology, 36 Nakhimousky prosp. Moscow 117997, Russia

[2]Departments of Physics and Mathematics, Bar-Ilan University, Ramat-Gan 52900, Israel

(Received 5 October 2006 and in revised form 6 March 2007)

Drift of individual $\beta$-plane vortices confined to one layer of a two-layer fluid under the rigid-lid condition is considered. For this purpose, the theory of two-layer quasi-geostrophic singular vortices is employed. On a $\beta$-plane, any non-zonal displacement of a singular vortex results in the development of a regular flow. An individual singular $\beta$-plane vortex cannot be steady on its own: the vortex moves coexisting with a regular flow, be the drift steady or not. In this paper, both kinds of drift of a singular vortex are considered. A new steady exact solution is presented, a hybrid regular–singular modon. This hybrid modon consists of a dipole component and a circularly symmetric rider. The dipole is regular, and the rider is a superposition of the singular vortex and a regular circularly symmetric field. The unsteady drift of a singular vortex residing in one of the layers is considered under the condition that, at the initial instant, the regular field is absent. The development of barotropic and baroclinic regular $\beta$-gyres is examined. Whereas the barotropic and baroclinic modes of the singular vortex are comparable in magnitudes, the baroclinic $\beta$-gyres attenuate with time, making the trajectory of the vortex close to that of a barotropic monopole on a $\beta$-plane.

## 1. Introduction

The behaviour of localized vortices on a $\beta$-plane is a long-standing problem of geophysical fluid dynamics. The two main subjects in discussion are steadily translating vortical structures and unsteadily evolving individual vortices. In this paper, we address both issues by employing the concept of two-layer quasi-geostrophic singular vortices (Reznik & Kizner 2007). In both cases, the two-layer quasi-geostrophic model with a rigid-lid condition at the surface is used, and an individual singular vortex confined to one layer is considered. Owing to the $\beta$-effect, an individual singular vortex on its own is not a steady-state solution to the problem, and therefore must coexist with a regular velocity field superimposed on the velocity field associated with the singular vortex itself. The equations governing the cooperative evolution of a singular vortex and the regular background flow due to the $\beta$-effect are derived in § 2.

†Author to whom correspondence should be addressed: zinovyk@mail.biu.ac.il

Eddies in the atmosphere and oceans are often durable. Therefore, much attention has been given to vortical structures that travel steadily in the zonal direction, i.e. along latitude circles, without changing their shapes (see Flierl *et al.* 1980; Kizner 1984, 1997; Tribbia 1984; Verkley 1984; Reznik 1987; Nycander 1988; Kizner *et al.* 2002, 2003*a*, *b*; Khvoles, Berson & Kizner 2005 and the references therein). Vortical configurations of this type are commonly referred to as modons.

The simplest $\beta$-plane modon is a dipolar structure, whose translational movement is due to the interaction between the vortices constituting the dipole (Larichev Reznik 1976*a*). In fact, any modon must contain a dipole or, more generally, an antisymmetric component (Reznik 1987). The role of the antisymmetric component in the modon translation is similar to that of a dipole; therefore, we frequently use the term 'dipole' component instead of 'antisymmetric' component. The presence of a component symmetric about the axis of the modon propagation is also possible. If the symmetric component is sufficiently strong, it can mask the dipole component (which is, probably, the case in durable atmospheric and oceanic eddies). The nonlinear self-interaction of the symmetric component enters the equation that describes the dipole. Therefore, generally, the symmetric component affects the dipole component and the translation speed of the modon as a whole (Kizner *et al.* 2002, 2003*a,b*; Kizner 2006). Modon solutions marked by the self-interaction of the symmetric component, the so-called elliptical baroclinic modons, were suggested by Kizner *et al.* (2003*a*). In the particular case where self-interaction of the symmetric component vanishes, this component can be arbitrarily strong and does not influence the dipole component and the modon translation speed. Such a symmetric component is colloquially referred to as a 'rider'. This situation occurs, for example, in the solutions with circularly symmetric baroclinic modes (Flierl *et al.* 1980; Kizner 1984, 1997).

Steadily translating ensembles of singular $\beta$-plane vortices have been considered in a number of papers (e.g. Reznik 1992; Gryanik 1986, 1988; Flierl 1987; Gryanik, Borth & Olbers 2004). In these vortical configurations, the amplitudes and coordinates of singular vortices are specially fitted to afford a steady translation of the ensemble without generation of any regular flow in addition to the flow associated with the singular vortices. Such a solution can be called a singular modon. Obviously, the simplest singular modon is a dipole consisting of two singular vortices of opposite signs. However, can a $\beta$-plane 'hybrid' modon solution be constructed, in which a steady flow induced by an individual singular vortex coexists with a steady regular flow? An approximate barotropic modon solution, where one singular vortex is equilibrated by a localized regular component was suggested by Reznik (1986). In this paper, we present an exact two-layer hybrid modon solution (§ 3). The solution is a sum of a regular dipole and a circular rider, which consists of one upper-layer singular vortex and a regular circularly symmetric component. The total angular momentum of the rider is zero. A characteristic property of this modon solution is its smoothness, i.e. the continuity of the streamfunction, velocity and potential vorticity in each layer everywhere except for the point where the singular vortex locates. Smoothness is an important feature of a modon, because numerical experiments revealed that smooth modons can be much more durable than modons with non-smooth riders (Kizner *et al.* 2002, 2003*a*).

The behaviour of an individual monopolar vortex differs from that of a modon. A study of non-stationary evolution of a localized vortex on the $\beta$-plane is another objective of our work. On the $f$-plane, an axisymmetric vortex is stationary. The $\beta$-effect and nonlinearity induce the development of a secondary dipolar circulation in the vicinity of the vortex. This secondary circulation, known as $\beta$-gyres, forces the vortex to move along a curved trajectory. The form of this trajectory depends on the sense of rotation of the vortex: a cyclone travels northwestward, and an anticyclone southwestward. Development of the $\beta$-gyres and their effect on barotropic cyclones and anticyclones were thoroughly examined both analytically (Reznik & Dewar 1994; Sutyrin & Flierl 1994; Reznik, Grimshaw & Benilov 2000) and numerically (Sutyrin *et al.* 1994).

The dynamics of baroclinic vortices are much more complicated and are still not clearly understood. Most studies have addressed the evolution of a fully baroclinic two-layer monopole, a vortex that initially does not contain any barotropic modes. We assign such a vortical structure to individual baroclinic vortices, even though, formally, it can be regarded as a pair of coaxial vortices. The generation of baroclinic $\beta$-gyres plays an important role in the evolution of such a structure, at least in the early stage. For example, when two coaxial point vortices opposite in sign reside in different layers, the baroclinic $\beta$-gyres incline the initially vertical axis of the vortex by shifting the cyclone to the north and the anticyclone to the south (Reznik, Grimshaw & Sriskandarajah 1997; Reznik & Kizner 2007, § 3.4.2). The subsequent evolution of this baroclinic structure differs fundamentally from that of an individual barotropic vortex (which propagates mainly westwards). Setting in of the meridional separation between the cyclone and anticyclone initiates their interaction. This results in an eastward drift of the vortex pair as a whole. The latter is consistent with numerical simulations, which demonstrated the ability of a fully baroclinic distributed monopole to eventually transform into an eastward-propagating baroclinic modon (McWilliams & Flierl 1979; Mied & Lindemann 1982; Kizner *et al.* 2002).

An important question arises as to how the above scenario changes when the initial vortex is neither fully baroclinic nor purely barotropic, but contains both modes. Reznik *et al.* (1997) conjectured that the barotropic component, provided it is sufficiently strong, might dominate the long-term dynamics of such a vortex. Here, we consider the unsteady evolution of an individual vortex confined to the upper layer (§ 4). Obviously, such a vortex contains both the barotropic and baroclinic modes that are comparable in magnitudes. Assuming the regular field to be zero at the initial instant, we examine the development of the barotropic and baroclinic regular $\beta$-gyres at subsequent times and show that the baroclinic $\beta$-gyres attenuate with time. Therefore, the trajectory of the vortex becomes close to that of a barotropic monopole on a $\beta$-plane.

The results of the work are summarized and discussed in § 5. Some cumbersome mathematical details are provided in Appendices A and B.

## 2. Basic equations

We depart from the well-known equations of conservation of the quasi-geostrophic potential vorticity (PV) in a two-layer fluid of constant depth with a rigid-lid condition at the surface:

$$\frac{\partial \Pi_i}{\partial t} + J(\psi_i, \Pi_i) = 0, \quad \Pi = q_i + \beta y, \quad i = 1, 2. \qquad (2.1a)$$

Here, subscripts $i = 1, 2$ are indices of the first (upper) and second (lower) layers; $\psi_i$, $\Pi_i$ and $q_i$ are the streamfunction, PV, and intrinsic vorticity in layer *i*, respectively. The intrinsic vorticities are defined by the following equations:

$$q_1 = \nabla^2\psi_1 + \Lambda_1(\psi_2 - \psi_1), \quad q_2 = \nabla^2\psi_2 + \Lambda_2(\psi_1 - \psi_2). \qquad (2.1b, c)$$

In (2.1*b*, *c*), $\Lambda_1 = f_0^2/g'H_1$ and $\Lambda_2 = f_0^2/g'H_2$, where the constants $f_0$ and $\beta$ are the reference value and northward gradient of the Coriolis parameter, $g' = g(\rho_2 - \rho_1)/\rho_2$ is the reduced gravity, $H_i$ and $\rho_i$ are the mean depth and fluid density in layer *i*.

A unit singular vortex confined to the upper layer and located at the origin is determined by the following equations:

$$\nabla^2\psi^u_{1,s} + \Lambda_1\left(\psi^u_{2,s} - \psi^u_{1,s}\right) - p^2\psi^u_{1,s} = \delta(x)\delta(y), \tag{2.2a}$$

$$\nabla^2\psi^u_{2,s} + \Lambda_2\left(\psi^u_{1,s} - \psi^u_{2,s}\right) - p^2\psi^u_{1,s} = 0. \tag{2.2b}$$

Here, $x$ and $y$ are the eastward and northward coordinates, respectively; $\delta(\,)$ is Dirac's delta-function; $\psi^u_{i,s}$ is the streamfunction of the flow induced in layer $i$ by the unit singular vortex located in layer 1; $p$ is an arbitrary positive constant, unless otherwise stated (Reznik & Kizner 2007, § 2.3). Equations (2.2) imply:

$$\psi^u_{1,s} = -\frac{1}{2\pi}\left(\alpha_1 K_0(pr) + \alpha_2 K_0(p_\Lambda r)\right), \quad \psi^u_{2,s} = -\frac{\alpha_1}{2\pi}\left(K_0(pr) - K_0(p_\Lambda r)\right), \tag{2.3a, b}$$

where $p_\Lambda^2 = p^2 + \Lambda_1 + \Lambda_2; \alpha_i = H_i/(H_1 + H_2)$; $r$ is the polar radius; $K_m()$ and $I_m()$ are the $m$-order modified Bessel functions of their arguments. The streamfunction $\psi^u_{1,s}$ has a logarithmic singularity at $r = 0$, whereas the streamfunction $\psi^u_{2,s}$ is regular throughout the $(x, y)$-plane.

To consider a flow that contains both the regular and singular components, the streamfunction in layer $i$ is represented as:

$$\psi_i = \psi_{i,r} + \psi_{i,s}, \quad i = 1, 2, \tag{2.4}$$

where $\psi_{i,r}$ is the streamfunction of the regular flow in layer $i$, and

$$\psi_{1,s} = A\psi^u_{1,s}(|\boldsymbol{r} - \boldsymbol{r}_0|), \quad \psi_{2,s} = A\psi^u_{2,s}(|\boldsymbol{r} - \boldsymbol{r}_0|), \tag{2.5}$$

are the streamfunctions of the flows produced in layers 1 and 2 by a singular vortex that has a constant amplitude $A$ and moves along a trajectory $\boldsymbol{r} = \boldsymbol{r}_0(t) = (x_0(t), y_0(t))$. Substitution of (2.3)–(2.5) into (2.1) yields the following equations that govern the evolution of the regular field interrelated with the motion of the singular vortex:

$$\frac{\partial}{\partial t}(q_{i,r} + p^2\psi_{i,s} + \beta y) + J(\psi_{i,r} + \psi_{i,s}, q_{i,r} + p^2\psi_{i,s} + \beta y) = 0, \quad i = 1, 2. \tag{2.6a}$$

$$\dot{x}_0 = -\left.\frac{\partial\psi_{1,r}}{\partial y}\right|_{\boldsymbol{r}=\boldsymbol{r}_0}, \quad \dot{y}_0 = \left.\frac{\partial\psi_{1,r}}{\partial x}\right|_{\boldsymbol{r}=\boldsymbol{r}_0} \tag{2.6b, c}$$

(for a number of singular vortices residing in both layers these equations were derived by Reznik & Kizner 2007, § 2.2). The variables $q_{1,r}$ and $q_{2,r}$ in (2.6*a*) are defined as

$$q_{1,r} = \nabla^2\psi_{1,r} + \Lambda_1(\psi_{2,r} - \psi_{1,r}), \quad q_{2,r} = \nabla^2\psi_{2,r} + \Lambda_2(\psi_{1,r} - \psi_{2,r}). \tag{2.7a, b}$$

## 3. Hybrid modon

In this section, we concern ourselves with the construction of a hybrid two-layer modon solution that incorporates both singular and regular components. The singular component is represented by an upper-layer singular vortex (equations (2.3) and (2.5)) located in the modon centre. The regular field is made up of a dipole and a circularly symmetric monopole. The regular dipole component produces the steady eastward translation of the modon, whereas the regular monopole equilibrates the singular vortex yielding zero total angular momentum of the modon. The latter is a necessary condition for the existence of a modon (Flierl *et al.* 1980, 1983).

The streamfunctions of a modon that travels along the $x$-axis at a constant speed $U$ can be represented as:

$$\psi_i = \psi_{i,r}(x - Ut, y) + \psi_{i,s}(x - Ut, y), \tag{3.1}$$

where $i = 1, 2$; and $\psi_{i,s}$ are given by (2.5) with $\boldsymbol{r}_0 = (Ut, 0)$. In a co-moving frame of reference (attached to the modon), (2.6) become:

$$J(\psi_{i,r} + \psi_{i,s} + Uy, q_{i,r} + p^2\psi_{i,s} + \beta y) = 0, \quad U = \left.\frac{\partial \psi_{1,r}}{\partial y}\right|_{r=0}. \tag{3.2a, b}$$

Following Larichev & Reznik (1976*a*) and Flierl *et al.* (1980), we assume that a circular contour (separatrix) $r = a$ exists, dividing the $(x, y)$-plane into two domains, the exterior and interior. The interior domain, $r < a$, is characterized by, at least in one of the layers, being filled with closed streamlines – contours of the full co-moving streamfunction $\Psi_i = \psi_{i,r} + \psi_{i,s} + Uy$. In the exterior domain, $r > a$, the streamlines are open in both layers.

As seen from (2.3), $\psi_{i,s}|_{r\to\infty} = 0$. Since a modon is a localized vortical structure, we require that $\psi_{i,r}|_{r\to\infty} = 0$. Under these conditions, in the exterior region, (3.2*a*) reduces to:

$$q_{i,r} + p^2\psi_{i,s} + \beta y = \frac{\beta}{U}(\psi_{i,r} + \psi_{i,s} + Uy), \quad r > a, \quad i = 1, 2, \tag{3.3a}$$

(cf. Flierl *et al.* 1980). Regarding the interior region, (3.2*a*) means that, in each layer, there is a functional relation between the potential vorticity, $\Pi_i$, and the full co-moving streamfunction, $\Psi_i$:

$$q_{i,r} + p^2\psi_{i,s} + \beta y = F_i(\psi_{i,r} + \psi_{i,s} + Uy), \quad r < a, \quad i = 1, 2, \tag{3.3b}$$

where $F_i()$ is some differentiable function.

In the upper layer, the left-hand side of (3.3*b*) contains a singularity at $r = 0$. The simplest way to cancel this singularity is to set $p^2 = \beta/U$ and $F_1(\Psi_1) = p^2\Psi_1$, i.e. to assume that the same linear relation between $\Pi_1$ and $\Psi_1$ holds in both the exterior and interior domains. In this case, throughout the $(x, y)$-plane, (3.2*a*) in the upper layer becomes:

$$q_{1,r} - p^2\psi_{1,r} = 0. \tag{3.4}$$

In the lower layer, in the interior domain we set $F_2$ to be linear, $F_2(\Psi_2) = -k^2\Psi_2 + D$, where $k^2$ and $D$ are some constant parameters that are to be specified. In fact, once the separatrix is chosen to be circular, linearity becomes the only possible choice (Kizner *et al.* 2003*a*). Thus, equations (3.3), which determine the regular component in layer 2, are:

$$q_{2,r} - p^2\psi_{2,r} = 0, \quad r > a, \tag{3.5a}$$

$$q_{2,r} + p^2\psi_{2,s} + \beta y = -k^2(\psi_{2,r} + \psi_{2,s} + Uy) + D, \quad r < a. \tag{3.5b}$$

To assure continuity of the streamfunction, velocity and vorticity fields, we seek a doubly continuously differentiable solution to (3.4), (3.5). This implies the following matching conditions at the separatrix $r = a$:

$$[\psi_{i,r}]_{r=a} = 0, \quad \left[\frac{\partial \psi_{i,r}}{\partial r}\right]_{r=a} = 0, \quad \left[\frac{\partial^2 \psi_{i,r}}{\partial r^2}\right]_{r=a} = 0, \quad i = 1, 2, \tag{3.6}$$

where the bracket symbol [ ] denotes the jump of a function at the contour $r = a$.

To avoid the difficulties caused by the interplay of the functions $\psi_{1,r}$ and $\psi_{2,r}$ in the interior domain $r < a$ (see (3.4), (3.5*b*) and (2.7)), the normal-mode variables, $\bar{\psi}_{1,r}$ and $\bar{\psi}_{2,r}$, are introduced. These new variables defined as linear combinations of $\psi_{1,r}$ and $\psi_{2,r}$,

$$\bar{\psi}_{i,r} = \psi_{1,r} + \bar{\alpha}_i\psi_{2,r}, \quad i = 1, 2, \tag{3.7}$$

satisfy the following decoupled equations

$$\nabla^2\bar{\psi}_{i,r} + k_i^2\bar{\psi}_{i,r} = -\bar{\alpha}_i[(k^2+p^2)\psi_{2,s} - D + (k^2U+\beta)y], \tag{3.8}$$

where

$$k_i^2 = -(\Lambda_1 + p^2) + \bar{\alpha}_i\Lambda_2, \tag{3.9}$$

and $\bar{\alpha}_i$ are roots of the quadratic equation in $\bar{\alpha}$,

$$\bar{\alpha}^2 - \frac{1}{\Lambda_2}(p^2 + k^2 + \Lambda_1 - \Lambda_2)\,\bar{\alpha} - \frac{\Lambda_1}{\Lambda_2} = 0. \tag{3.10}$$

According to (3.9) and (3.10), $k_1^2$ and $k_2^2$ obey the relationship:

$$\left(k_1^2 + \Lambda_1 + p^2\right)\left(k_2^2 + \Lambda_1 + p^2\right) = -\Lambda_1\Lambda_2, \tag{3.11}$$

therefore, at least one of $k_i^2$ is negative. For definiteness, we assume that $k_1^2 < k_2^2$ and $k_1^2 < 0$. Under these assumptions, as follows from the matching conditions (3.6), parameter $k_2^2$ must be positive (see Appendix A), i.e.

$$k_1^2 < 0, \quad k_2^2 > 0. \tag{3.12}$$

We assume the solution of the interior problem to consist of a circularly symmetric component, $\bar{\psi}_{i,r}^{(0)}(r)$, and a component $\bar{\psi}_{i,r}^{(d)}(r)\sin\theta$, which is antisymmetric relative to the $x$-axis:

$$\bar{\psi}_{i,r} = \bar{\psi}_{i,r}^{(0)}(r) + \bar{\psi}_{i,r}^{(d)}(r)\sin\theta. \tag{3.13}$$

Substitution of (3.13) into (3.8) provides the following equations for $\bar{\psi}_{i,r}^{(0)}(r)$ and $\bar{\psi}_{i,r}^{(d)}(r)$:

$$\nabla^2\bar{\psi}_{i,r}^{(0)} + k_i^2\bar{\psi}_{i,r}^{(0)} = -\bar{\alpha}_i(k^2+p^2)\psi_{2,s} + \bar{\alpha}_i D, \tag{3.14a}$$

$$\nabla^2\bar{\psi}_{i,r}^{(d)} + k_i^2\bar{\psi}_{i,r}^{(d)} = -\bar{\alpha}_i(k^2U+\beta)y. \tag{3.14b}$$

Taking into account relationships (2.3) and (2.5), the solutions to (3.14) can be written as

$$\bar{\psi}_{i,r}^{(0)} = \frac{\alpha_1 A}{2\pi}\frac{\bar{\alpha}_i(p^2+k^2)}{(p^2+k_i^2)(p_\Lambda^2+k_i^2)}\bar{g}_i + C_i G_0(|k_i|r) + \frac{\bar{\alpha}_i}{k_i^2}D, \tag{3.15a}$$

$$\bar{g}_i = \left(p_\Lambda^2 + k_i^2\right)K_0(pr) - \left(p^2 + k_i^2\right)K_0(p_\Lambda r) + \left(p_\Lambda^2 - p^2\right)Z_0(|k_i|\,r), \tag{3.15b}$$

$$\bar{\psi}_{i,r}^{(d)} = \left[A_i^{(1)}G_1(|k_i|\,r) - \frac{\bar{\alpha}_i(k^2U+\beta)r}{k_i^2}\right]\sin\theta. \tag{3.15c}$$

with $C_i$, $A_i^{(1)}$ being constants that will be specified later. The remaining notations are:

$$G_m(|k_1|r) = I_m(|k_1|r), \quad G_m(|k_2|r) = J_m(k_2r), \quad m = 0,\ 1, \tag{3.16a}$$

$$Z_0(|k_1|r) = -K_0(|k_1|r), \quad Z_0(|k_2|r) = \frac{1}{2}\pi Y_0(k_2r), \tag{3.16b}$$

where $J_m(\ )$ and $Y_m(\ )$ are the $m$-order Bessel functions of the first and second kinds, respectively. It can readily be checked that, despite the singularity of the functions $K_0$ and $Y_0$ at $r = 0$, the functions $\bar{g}_i$ and, hence, $\bar{\psi}_{i,r}^{(0)}$, are regular.

In the exterior domain, $r > a$, (3.4) and (3.5$a$) are valid. Thus, the solution here is given by (3.13) with

$$\bar{\psi}_{i,r}^{(0)} = (1+\bar{\alpha}_i)B_0K_0(pr) + (\alpha_2 - \alpha_1\bar{\alpha}_i)B_0^{(\Lambda)}K_0(p_\Lambda r), \tag{3.17a}$$

$$\bar{\psi}_{i,r}^{(d)} = [(1+\bar{\alpha}_i)B_1K_1(pr) + (\alpha_2 - \alpha_1\bar{\alpha}_i)B_1^{(\Lambda)}K_1(p_\Lambda r)]\sin\theta, \tag{3.17b}$$

where the constant coefficients $B_0$, $B_1$, $B_0^{(\Lambda)}$ and $B_1^{(\Lambda)}$ are to be determined.

Given $U$ (or $a$), we can determine the parameters $k_1, k_2, \bar{\alpha}_1, \bar{\alpha}_2, k$ and $a$ (or $U$), and the coefficients appearing in (3.15$a,c$) and (3.17). Because the calculations are cumbersome, for the moment we present only their outline and results; for a detailed analysis see Appendix A. To specify the coefficients $A_i^{(1)}, B_0, B_0^{(\Lambda)}, B_1, B_1^{(\Lambda)}$ and $C_i$, we substitute (3.13) into (3.2$b$) and in the matching conditions (3.6) rewritten in terms of the normal-mode variables (3.7). As a result, a system of linear equations in $A_i^{(1)}, B_1, B_1^{(\Lambda)}, B_0, B_0^{(\Lambda)}$ and $C_i$ is obtained. The solvability conditions for the subsystem in $A_i^{(1)}, B_1, B_1^{(\Lambda)}$, along with (3.9)–(3.11), impose constraints on the parameters $k_1, k_2, \bar{\alpha}_1, \bar{\alpha}_2, k, U$ and $a$, so that only one of these parameters is free. By fixing, for example, the modon translation speed $U$, we can determine the modon radius $a$, the parameters $k_i, \bar{\alpha}_i$ and $k$ and, hence, the coefficients $A_i^{(1)}, B_1, B_1^{(\Lambda)}$ in (3.15$c$) and (3.17$b$). The equations determining $A$, $D$, $B_0$, $B_0^{(\Lambda)}$ and $C_i$ are linearly dependent, therefore, the amplitude $A$ of the singular vortex is arbitrary, whereas the coefficients $D$, $B_0$, $B_0^{(\Lambda)}$ and $C_i$ are proportional to $A$. Further, given $\bar{\alpha}_i$ and the functions $\bar{\psi}_{i,r}^{(0)}$ and $\bar{\psi}_{i,r}^{(d)}$, the regular streamfunctions $\psi_{i,r}$ are found from (3.7) and (3.13):

$$\psi_{i,r} = \psi_{i,r}^{(0)}(r) + \psi_{i,r}^{(d)}(r)\sin\theta. \tag{3.18a}$$

In (3.18$a$), the circularly symmetric rider $\psi_{i,r}^{(0)}(r)$, and the dipole component $\psi_{ir}^{(d)}(r)$ are given by the following formulae

$$\psi_{1,r}^{(0)} = \frac{\bar{\alpha}_2\bar{\psi}_{1,r}^{(0)} - \bar{\alpha}_1\bar{\psi}_{2,r}^{(0)}}{\bar{\alpha}_2 - \bar{\alpha}_1}, \quad \psi_{2,r}^{(0)} = \frac{\bar{\psi}_{2,r}^{(0)} - \bar{\psi}_{1,r}^{(0)}}{\bar{\alpha}_2 - \bar{\alpha}_1}, \tag{3.18b, c}$$

$$\psi_{1,r}^{(d)} = \frac{\bar{\alpha}_2\bar{\psi}_{1,r}^{(d)} - \bar{\alpha}_1\bar{\psi}_{2,r}^{(d)}}{\bar{\alpha}_2 - \bar{\alpha}_1}, \quad \psi_{2,r}^{(d)} = \frac{\bar{\psi}_{2,r}^{(d)} - \bar{\psi}_{1,r}^{(d)}}{\bar{\alpha}_2 - \bar{\alpha}_1}. \tag{3.18d, e}$$

The structure of the solution depends on the parameter $k_2$, which is subject to the restriction:

$$j_{1,n} \leqslant k_2 a \leqslant j_{2,n}, \tag{3.19}$$

with $j_{1,n}$ and $j_{2,n}$ being the $n$th roots of the first- and second-order Bessel functions $J_1$ and $J_2$, respectively ($m = 1, 2, \ldots$). Theoretically, the modon's structure strongly depends on $n$ since, because of the alternating behaviour of Bessel functions $J_m$ in (3.16$a$), the antisymmetric component of the solution contains $2n$ regions of closed streamlines rather than two ones as in dipoles. The simplest structure should be obtained at $n = 1$. In this case, the antisymmetric component must be a dipole, i.e. a pair of vortices of opposite signs. We can guess that the solutions with $n > 1$ (if they exist) are unstable (Kizner & Berson 2000). A numerical examination of the cases $n = 1$ and $n = 2$ shows that at $n = 1$ a solution does exist, whereas at $n = 2$ does not.

As seen in figure 1, where the modon dispersion relation (i.e. size *vs.* speed) is shown, the modon radius $a$ decreases monotonically as the translation speed $U$ grows. Both $a$ and $U$ are non-dimensional, being scaled with the Rossby deformation radius

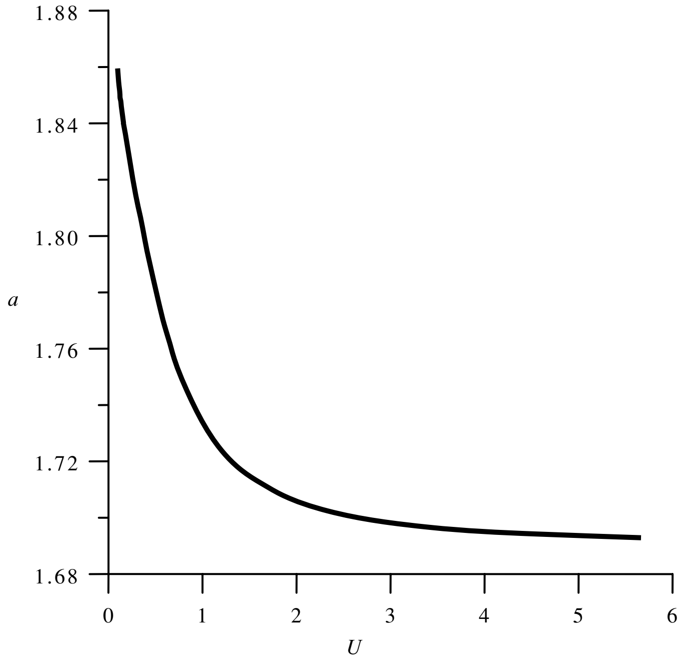


FIGURE 1. Dispersion relationship for a hybrid modon at $H_1:H_2=1:4$. The modon radius $a$ and the translation speed $U$ are scaled with $R_d=\sqrt{\Lambda_1+\Lambda_2}$ and $\beta R_d^2$, respectively.

$R_d=\sqrt{\Lambda_1+\Lambda_2}$ and $\beta R_d^2$, respectively; the stratification assumed in this example is $H_1:H_2=\alpha_1:\alpha_2=1:4$.

The amplitude of the circularly symmetric rider is arbitrary and is determined by the magnitude $A$ of the singular vortex. As explained in § 1, such a rider does not affect the modon transition. In figure 2, the radial profiles of the singular- and regular-component streamfunctions of the circularly symmetric rider are shown for the case $A>0$, i.e. when the singular vortex is a cyclone. In both layers, the singular vortex induces rotation of the same sense, and in the upper layer (where the singular vortex resides) the motion is much stronger than in the lower layer (figure 2*a*, *b*). The total angular momentum of any modon must be zero (see Flierl *et al.* 1980, 1983). Regarding our hybrid solution this implies that

$$\int(\alpha_1\psi_{1,s}+\alpha_2\psi_{2,s})\mathrm{d}x\mathrm{d}y+\int\left(\alpha_1\psi_{1,r}^{(0)}+\alpha_2\psi_{2,r}^{(0)}\right)\mathrm{d}x\mathrm{d}y=0, \tag{3.20}$$

where the integration is carried out over the entire $(x, y)$-plane. At $A>0$, both $\psi_{1,s}$ and $\psi_{2,s}$ are negative, and the second integral on the left-hand side of (3.20) is positive. Thus, the regular component of the rider is predominantly anticyclonic. In fact, the regular component of the rider is anticyclonic in both layers and, unlike the singular component, is more or less of the same magnitude in both layers (figure 2*c*). Evidently, in the upper layer, the singular component, $\psi_{1,s}$, is dominant in the rider, whereas in the lower layer, the regular component $\psi_{2,r}^{(0)}$ is dominant.

The dipole component of the hybrid modon is shown in figure 3. An important feature of the dipole is that the amplitude of the streamfunction in the lower-layer is much larger (almost by the order of magnitude) than in the upper layer. This can be explained by considering the barotropic component of the modon. It is this barotropic

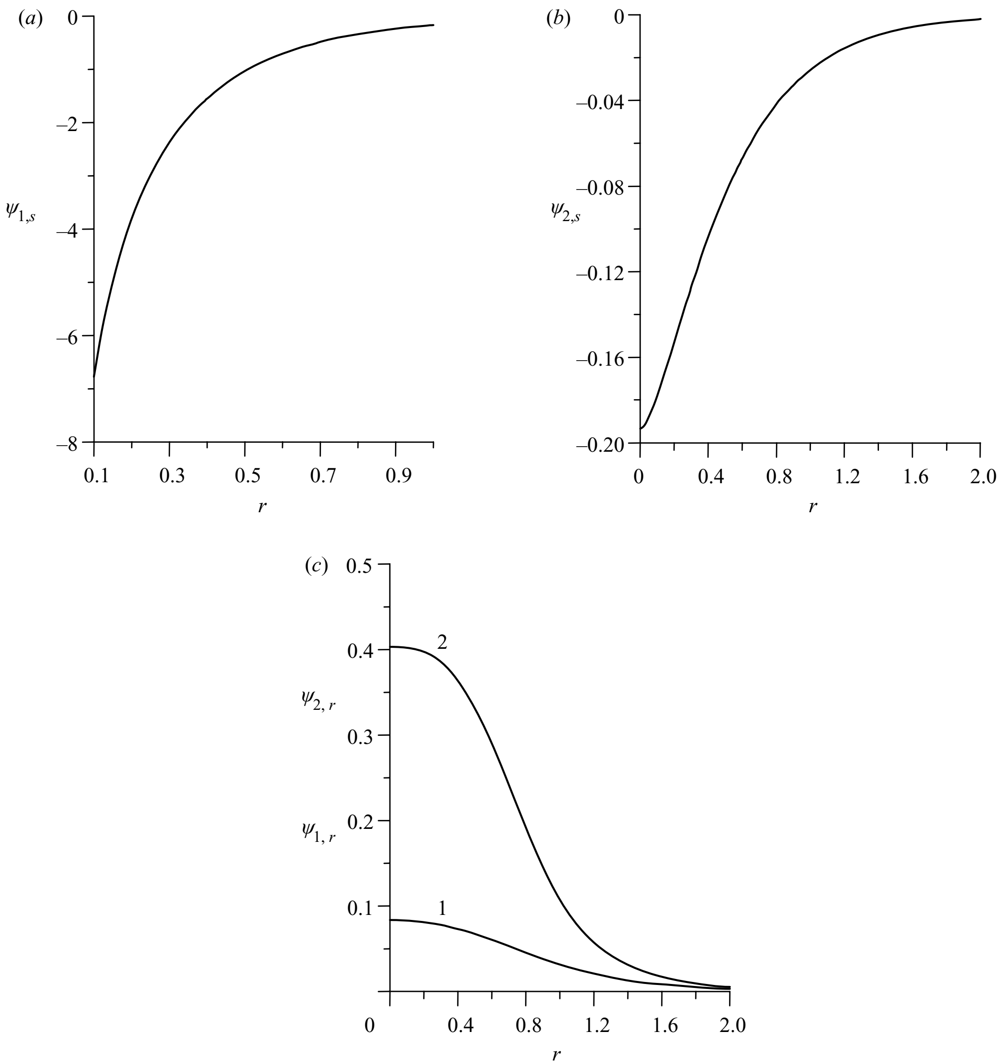


FIGURE 2. Rider component of a hybrid modon. Profiles of the rider streamfunctions at $H_1\colon H_2 = 1{:}4$ and $A = 1$. (*a*) Upper-layer singular streamfunction, $\psi_{1,s}$; (*b*) lower-layer singular streamfunction, $\psi_{2,s}$; (*c*) regular streamfunctions $\psi_{1,r}^{(0)}$ and $\psi_{2,r}^{(0)}$ in the layers: 1, upper-layer; 2, lower-layer.

dipole component that serves as an 'engine' causing the eastward self-propulsion of the modon as a whole. A direct calculation shows that the velocity induced by the barotropic mode of the dipole (at the point where the singular vortex occurs) exceeds the translation speed $U$. Therefore, to satisfy condition (3.2*b*), the dipole $\bar{\psi}_{i,r}^{(d)}(r)\sin\theta$ should contain a baroclinic mode that depresses the upper-layer dipole and makes it propel the singular vortex with the speed $U$. In contrast, in the lower layer, the dipole is enhanced by the baroclinic dipole.

The key issue in the construction of an exact hybrid modon solution was the elimination of singularity in (3.3*b*) at $i = 1$, which resulted in (3.4). Such elimination is impossible in the framework of a barotropic model. Accordingly, so far only an approximate barotropic hybrid modon solution had been found (Reznik 1986).

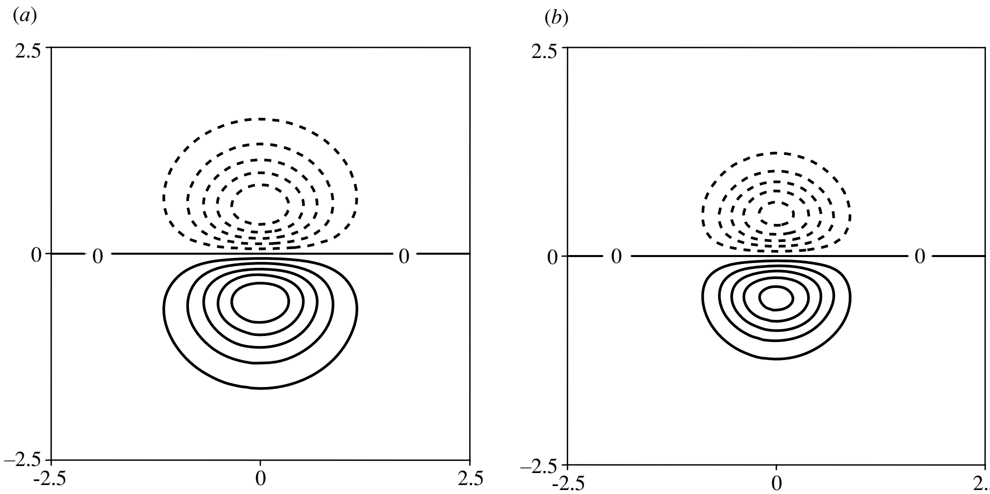


FIGURE 3. Dipole component of the hybrid modon. Contours of the dipole streamfunctions in the layers at $H_1 : H_2 = 1:4$, $a = 1.8$. Solid lines, positive (anticyclone); dashed lines, negative (cyclone). (*a*) Upper layer, $\max|\psi_{1,r}^{(d)}| \approx 0.3$, contour interval 0.05; (*b*) lower layer, $\max|\psi_{1,r}^{(d)}| \approx 2.18$, contour interval 0.4.

## 4. Non-stationary evolution of an individual singular vortex

The subject of this section will be the motion of an intense upper-layer individual singular vortex associated with the development of a regular flow. Let the regular field be absent at the initial instant. In this case, at $t = 0$, the streamfunctions in the layers are given by (2.5). At subsequent times, in response to meridional displacement of the singular vortex, some regular flow arises because of the $\beta$-effect, and the singular vortex starts moving along a certain path $\boldsymbol{r} = \boldsymbol{r}_0 = (x_0(t), y_0(t))$ with the speed $\boldsymbol{U} = (U, V)$, where $U = \dot{x}_0(t)$ and $V = \dot{y}_0(t)$. At the very beginning, a singular vortex located in one of the layers behaves similarly to a purely barotropic vortex: a cyclone moves northward and an anticyclone southward (Reznik & Kizner 2007, § 3.4.1). To study the motion of the vortex at later stages, the development of the $\beta$-gyres should be examined. Thus, we arrive at an initial-value problem, which is determined by (2.6) supplemented with the initial conditions $\psi_{i,r}|_{t=0} = 0$.

To facilitate the subsequent analysis, equations (2.6) are rewritten in non-dimensional variables in the co-moving frame of reference attached to the singular vortex:

$$\frac{\partial q_{i,r}}{\partial t} + \frac{\partial \psi_{i,s}}{\partial x} + J(\psi_{i,s}, q_{i,r}) + p^2 J(\psi_{i,r} + Uy - Vx, \psi_{i,s}) + \varepsilon \left[ \frac{\partial \psi_{i,r}}{\partial x} + J(\psi_{i,r} + Uy - Vx, q_{i,r}) \right] = 0, \tag{4.1a}$$

$$\dot{x}_0 = U = - \left. \frac{\partial \psi_{1,r}}{\partial y} \right|_{r=0}, \ \dot{y}_0 = V = \left. \frac{\partial \psi_{1,r}}{\partial x} \right|_{r=0}. \tag{4.1b, c}$$

Here the space variables, time and velocity are scaled with the Rossby radius, $R_d = \sqrt{\Lambda_1 + \Lambda_2}$, typical advective time $2\pi R_d^2/A$, and $\beta R_d^2$, respectively. Accordingly, the scale of the regular streamfunctions $\psi_{i,r}$ is $\beta R_d^3$. This scaling assures the balance between the terms $\partial q_{i,r}/\partial t$, $\beta(\partial \psi_{i,s}/\partial x)$ and $J(\psi_{i,s}, q_{i,r})$ in (2.6*a*). The reason for such a scaling is that the development of the regular flow is due to the $\beta$-effect and is induced by the meridional displacement of the singular vortex (see also Reznik 1992). In (4.1$a$),

$$\psi_{1,s} = -[\alpha_1 K_0(pr) + \alpha_2 K_0(p_A r)], \quad \psi_{2s} = -\alpha_1 [K_0(pr) - K_0(p_A r)], \tag{4.2$a, b$}$$

$$q_{1,r} = \nabla^2 \psi_{1,r} + \alpha_2(\psi_{2,r} - \psi_{1,r}), \quad q_{2,r} = \nabla^2 \psi_{2,r} + \alpha_1(\psi_{1,r} - \psi_{2,r}); \tag{4.2$c, d$}$$

parameter $p$ is non-dimensional (obtained by multiplication of the dimensional $p$ by $R_d$), $p_A^2 = 1 + p^2$, and $\varepsilon = 2\pi\beta R_d^3/A$ is the ratio of the typical drift speed $\beta R_d^2$ to the typical advective velocity $A/2\pi R_d$. We consider an intense vortex, in which case $\varepsilon$ is a small parameter:

$$\varepsilon \ll 1. \tag{4.3}$$

By eliminating the term with the factor $\varepsilon$, (4.1$a$) becomes:

$$\frac{\partial q_{i,r}}{\partial t} + \frac{\partial \psi_{i,s}}{\partial x} + J(\psi_{i,s}, q_{i,r}) + p^2 J(\psi_{i,r} + Uy - Vx, \psi_{i,s}) = 0. \tag{4.4}$$

Despite the approximation, equations (4.4) ($i = 1, 2$) are still too complicated. Therefore, we adopt another simplifying assumption:

$$p^2 \ll 1. \tag{4.5}$$

To find the meaning of condition (4.5), recall that the baroclinic component of the singular vortex (4.2$a, b$) is proportional to $K_0(p_A r)$ and the barotropic component to $-\alpha_1 K_0(pr)$. Thus, the space scale of the barotropic component, $1/p$, is assumed large, so that, in the initial state, the baroclinic mode decreases at infinity substantially faster than the barotropic mode.

Neglecting small terms in (4.4), we obtain

$$\frac{\partial(q_{i,r} + y)}{\partial t} + b_i \frac{\partial(q_{i,r} + y)}{\partial \theta} = 0, \tag{4.6}$$

where $\theta$ is the polar angle in the co-moving frame of reference, and

$$b_i = \frac{1}{r}\frac{\partial \psi_{i,s}}{\partial r}, \quad b_1 = \frac{1}{r}\left(\alpha_1 p K_1(pr) + \alpha_2 p_A K_1(p_A r)\right), \quad b_2 = \frac{\alpha_1}{r}\left(p K_1(pr) - p_c K_1(p_A r)\right). \tag{4.7$a$–$c$}$$

The derivation of the solution to (4.6) that satisfies the initial condition $q_{i,r}|_{t=0} = 0$ is straightforward:

$$q_{i,r} = -r(1 - \cos b_i t)\sin\theta - r \sin b_i t \cos\theta. \tag{4.8}$$

As seen from (4.8), in each layer, the regular vorticity field $q_{i,r}$ induced by the $\beta$-effect and nonlinearity appears as a dipole, i.e. a pair of $\beta$-gyres, whose axis, structure and magnitude vary with time.

To calculate the streamfunctions of these $\beta$-gyres, we decompose $\psi_{1,r}$ and $\psi_{2,r}$ into linear combinations of the regular barotropic and baroclinic modes, $\psi_{BT}$ and$\psi_{BC}$:

$$\psi_{1,r} = \psi_{BT} + \alpha_2 \psi_{BC}, \quad \psi_{2,r} = \psi_{BT} - \alpha_1 \psi_{BC}. \tag{4.9$a, b$}$$

Substitution of (4.9) into (4.2$c, d$) and (4.8) yields:

$$\psi_{BT} = \psi_{BT}^{(s)} \sin\theta + \psi_{BT}^{(c)} \cos\theta, \quad \psi_{BC} = \psi_{BC}^{(s)} \sin\theta + \psi_{BC}^{(c)} \cos\theta, \tag{4.10$a, b$}$$

where

$$\psi_{BT}^{(s)} = \frac{r}{2}\int_r^\infty r(1 - \alpha_1 \cos b_1 t - \alpha_2 \cos b_2 t)\mathrm{d}r + \frac{1}{2r}\int_0^r r^3(1 - \alpha_1 \cos b_1 t - \alpha_2 \cos b_2 t)\mathrm{d}r, \tag{4.11$a$}$$

$$\psi_{BT}^{(c)} = \frac{r}{2}\int_r^\infty r(\alpha_1 \sin b_1 t + \alpha_2 \sin b_2 t)\mathrm{d}r + \frac{1}{2r}\int_0^r r^3(\alpha_1 \sin b_1 t + \alpha_2 \sin b_2 t)\mathrm{d}r, \quad (4.11b)$$

$$\psi_{BC}^{(s)} = I_1(r)\int_r^\infty r^2 K_1(r)(\cos b_2 t - \cos b_1 t)\mathrm{d}r + K_1(r)\int_0^r r^2 I_1(r)(\cos b_2 t - \cos b_1 t)\mathrm{d}r, \quad (4.11c)$$

$$\psi_{BC}^{(c)} = I_1(r)\int_r^\infty r^2 K_1(r)(\sin b_1 t - \sin b_2 t)\mathrm{d}r + K_1(r)\int_0^r r^2 I_1(r)(\sin b_1 t - \sin b_2 t)\mathrm{d}r. \quad (4.11d)$$

Once the function $\psi_{1,r}$ is known, the drift speed of the vortex can be calculated based on (4.1*b*, *c*):

$$\dot{x}_0 = U = -\tfrac{1}{2}\int_0^\infty r[1 - (\alpha_1 + \alpha_2 r K_1(r))\cos b_1 t - \alpha_2(1 - rK_1(r))\cos b_2 t]\mathrm{d}r, \quad (4.12a)$$

$$\dot{y}_0 = V = \tfrac{1}{2}\int_0^\infty r[(\alpha_1 + \alpha_2 r K_1(r))\sin b_1 t + \alpha_2(1 - rK_1(r))\sin b_2 t]\mathrm{d}r. \quad (4.12b)$$

The development of the $\beta$-gyres is shown in figure 4 for the case $A > 0$ (cyclonic singular vortex). From this figure, we notice that the regular flow in each layer is a dipole that induces the northwestward drift of the singular vortex. The strength of the dipoles increases with increasing time. Therefore, the absolute values of each of the components of the total drift speed, $U$ and $V$, presented in figure 5 also grow with time, and the drift of the singular monopole accelerates. An important feature of this evolution is that, with the passage of time, the barotropic mode of the $\beta$-gyres enhances much faster than the baroclinic mode: by $t = 50$, the barotropic mode exceeds the baroclinic one by an order of magnitude. Long-term calculations and asymptotic analysis show that, at some moment, the growth of the baroclinic mode ceases; thereafter this component decays (see below).

To characterize the relative impacts of the barotropic and baroclinic components of the regular flow on the vortex drift, we decompose the drift speed determined by (4.12) into components due to the barotropic and baroclinic $\beta$-gyres:

$$(U, V) = (U_{BT}, V_{BT}) + (U_{BC}, V_{BC}). \quad (4.13)$$

These components, denoted by subscripts $BT$ and $BC$, will be referred to as the barotropic and baroclinic drift speeds, respectively. Equations (4.12) and (4.13) imply:

$$U_{BT} = -\tfrac{1}{2}\int_0^\infty r(1 - \alpha_1 \cos b_1 t - \alpha_2 \cos b_2 t)\mathrm{d}r, \quad V_{BT} = \tfrac{1}{2}\int_0^\infty r(\alpha_1 \sin b_1 t + \alpha_2 \sin b_2 t)\mathrm{d}r, \quad (4.14a, b)$$

$$U_{BC} = \frac{\alpha_2}{2}\int_0^\infty r^2 K_1(r)(\cos b_1 t - \cos b_2 t)\mathrm{d}r, \quad V_{BC} = \frac{\alpha_2}{2}\int_0^\infty r^2 K_1(r)(\sin b_1 t - \sin b_2 t)\mathrm{d}r. \quad (4.14c, d)$$

The evolution of the total drift speed and its barotropic and baroclinic components is shown in figure 5. The barotropic meridional speed component, $V_{BT}$, is close to the total meridional speed at all times; thus, the baroclinic component, $V_{BC}$, is negligible. At sufficiently large times the baroclinic zonal speed, $U_{BC}$, is also rather small, and the total zonal speed, $U$, becomes close to $U_{BT}$.

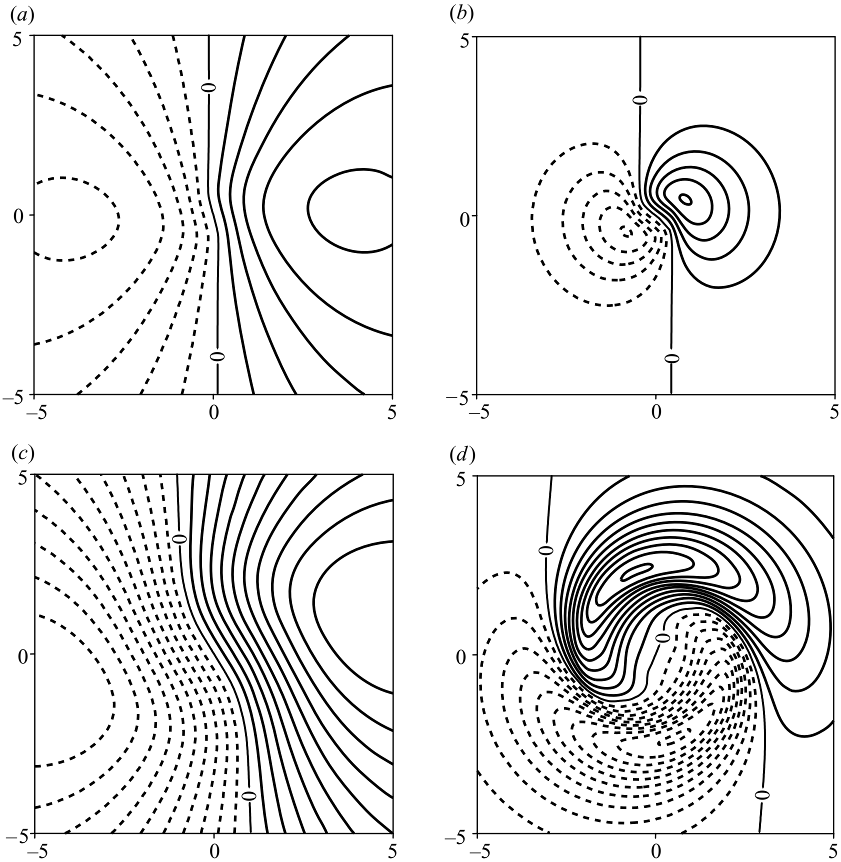


FIGURE 4. Barotropic and baroclinic $\beta$-gyres: contours of the barotropic and baroclinic streamfunctions, $\psi_{BT}$ and $\psi_{BC}$, at $H_1$:$H_2$ = 1:4. Solid and dashed lines as in figure 3. $(a, b)$, $t = 1$; $(c, d)$, $t = 50$. $(a)$ $\psi_{BT}$, $\max|\psi_{BT}| \approx 0.26$, contour interval 0.05; $(b)$ $\psi_{BC}$, $\max|\psi_{BC}| \approx 0.15$, contour interval 0.05; $(c)$ $\psi_{BT}$, $\max|\psi_{BT}| \approx 10.97$, contour interval 1; $(d)$ $\psi_{BC}$, $\max|\psi_{BC}| \approx 1.01$, contour interval 0.1.

Asymptotic estimates at large times confirm these conclusions. According to these estimates (Appendix B), the baroclinic $\beta$-gyres decay at large times and, consequently, the following asymptotics hold at any fixed $r$

$$U_{BC} = O\left(\frac{1}{t}\right), \quad V_{BC} = O\left(\frac{1}{t}\right), \quad t \to \infty. \tag{4.15}$$

$$\psi_{BC} = O\left(\frac{1}{t}\right), \quad t \to \infty. \tag{4.16}$$

On the contrary, the barotropic $\beta$-gyres build up at large times, and for any fixed $r$ we obtain:

$$U_{BT} = \frac{1}{p^2}\left(\tfrac{1}{2}\ln^2 t + \gamma \ln t\right) + O(1), \quad t \to \infty, \tag{4.17$a$}$$

$$V_{BT} = \frac{1}{p^2}\left(\frac{\pi}{2}\ln t - c_0\right) + O\left(\frac{\ln t}{t}\right), \quad t \to \infty, \tag{4.17$b$}$$

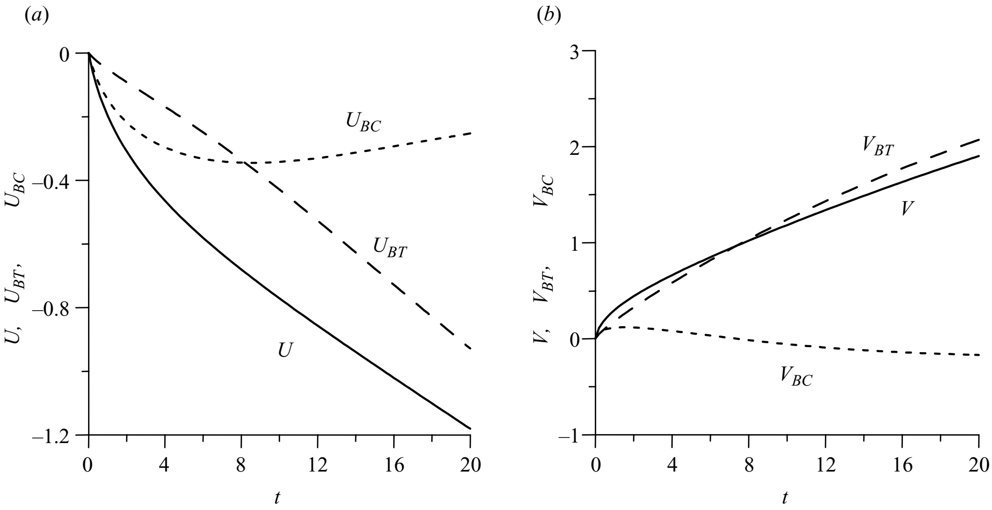


FIGURE 5. Temporal evolution of the vortex drift speed at $H_1 : H_2 = 1{:}4$ and $p = 0.3$ (non-dimensional). (*a*) Zonal speed $U$ and its components $U_{BT}$ and $U_{BC}$; (*b*) northward speed $V$ and its components $V_{BT}$ and $V_{BC}$. Subscripts $BT$ and $BC$ denote the speed components due to the barotropic and baroclinic $\beta$-gyres, respectively.

$$\psi_{BT} = r(-U_{BT}\sin\theta + V_{BT}\cos\theta) + O(1), \quad t \to \infty, \tag{4.18}$$

where $\gamma$ and $c_0$ are constants.

The above analysis shows that the $\beta$-gyres tend to become barotropic with the passage of time, and the resulting drift of the singular vortex becomes similar to the drift of a barotropic monopole: a cyclone moves northwestward, and an anticyclone southwestward. The baroclinic components of the $\beta$-gyres tend to incline the axis of the entire vortical structure, i.e. to increase the horizontal separation between the centres of the upper and lower vortices (defined as the distance between the location of the upper-layer singular vortex, and the point where the maximal absolute value of the lower-layer streamfunction is assumed). This effect of the baroclinic $\beta$-gyres attenuates with increasing time. The observed evolution of an individual singular vortex confined to one layer differs from that of a purely baroclinic singular vortex (see § 1). We believe this difference is due to the presence of a sufficiently strong barotropic component in the individual singular vortex.

## 5. Summary and discussion

To examine the interaction between an individual singular vortex and a regular flow in a two-layer fluid on a $\beta$-plane, we applied the theory of two-layer quasi-geostrophic singular vortices suggested in (Reznik & Kizner 2007). In particular, the equations were presented that govern the cooperative evolution of a singular vortex and the regular background flow under the rigid-lid condition. Although a singular vortex confined to the upper layer was considered, after interchanging indices 1 and 2, the results become applicable to the case when the singular vortex resides in the lower layer.

A new steady exact solution was obtained that can be categorized as a hybrid regular–singular modon. This hybrid modon consists of a dipole component and a circularly symmetric rider. The rider is a superposition of the upper-layer singular vortex and a regular circularly symmetric flow. In the upper layer, the singular component is dominant in the rider, whereas in the lower layer, the regular component prevails. The singular and regular components of the rider imply rotation in opposite directions, and the total angular momentum of the modon is zero. The dipole component of the modon in the lower-layer is much stronger than that in the upper-layer; this affords the advection of the singular vortex with the constant speed of the modon's translational motion. Thus, our hybrid modon can be considered as a model of apparently monopolar and nearly steady localized eddies occurring in the atmosphere and oceans.

An important property of the hybrid modon solution is its smoothness in the sense that the streamfunction in each layer is continuous up to the second derivatives everywhere except for the location of the singular vortex. Smooth regular dipole-plus-rider solutions on the $\beta$-plane were first suggested by Kizner (1984, 1997) for any stratification of the fluid. Numerical simulations ran with multi-layer versions of these solutions (Kizner *et al.* 2002, 2003*a*) revealed that such smooth modons are much more durable than the modons with non-smooth riders described by Flierl *et al.* (1980). This motivated our interest in looking for a solution with a continuous regular PV field. Baroclinicity of the flow, which supplies an additional degree of freedom to the problem, appears to be a key factor enabling the construction of the exact smooth hybrid modon solution. This is supported by the fact that, in the barotropic case, only an approximate hybrid modon solution has been found so far (Reznik 1986). Similarly, although asymptotic solutions were obtained both in the barotropic (Larichev & Reznik 1976*b*; Nycander 1988) and baroclinic (Kizner 1986*a*, *b*) cases, smooth exact regular modon solutions with riders were found only in a stratified fluid (Kizner 1984, 1988, 1997).

Non-stationary drift of a singular vortex in a stratified fluid on a $\beta$-plane depends significantly on the vertical structure of the vortex. This is because of the possible interaction between vortex elements residing at different depths. For example, if the vortex (whether singular or regular) in a two-layer fluid is initially a purely baroclinic monopole (i.e. a pair of coaxial vortices with zero net angular momentum), then, because of the $\beta$-effect, its axis inclines, the upper and lower vortices start interacting, and eventually the vortex transforms into an eastward-travelling modon (McWilliams & Flierl 1979; Mied & Lindemann 1982; Reznik *et al.* 1997; Kizner *et al.* 2002). In this paper, we considered the motion of a singular vortex that resides in one layer of a two-layer fluid. From the beginning, such a vortex is not purely baroclinic, but contains both baroclinic and barotropic modes which are comparable in magnitude. The presence, in the initial state, of a substantial barotropic component (along with the baroclinic one) makes the upper and lower flows co-rotating. This changes the vortex evolution considerably compared to the above scenario.

We assume the regular field to be zero at the initial instant, and examine the development of the regular $\beta$-gyres at subsequent times. The main result of this analysis is that the influence of the baroclinic component of the $\beta$-gyres on the vortex drift attenuates, and the $\beta$-gyres tend to become barotropic with increasing time. Accordingly, the trajectory of the vortex appears qualitatively close to the track of a barotropic monopole on a $\beta$-plane.

G. R. gratefully acknowledges the hospitality extended to him by Bar-Ilan University during his stay in Israel, and the support from Russian Foundation for Basic Research, Grant 05-05-64212. Z. K. acknowledges the support from Israel Science Foundation, 628/06. The authors thank the Centre for Academic and Educational Relations of the Humanities, Hebrew University, for partial support of this research.

## Appendix A. Fulfilment of the matching conditions

Until the sign of $k_2^2$ is specified, the solution to (3.14) can be written in the form of (3.15), where

$$G_n(|k_2|\,r) = \begin{cases} -I_n(|k_2|\,r), & k_2^2 < 0, \\ J_n(k_2 r), & k_2^2 > 0, \end{cases} \quad n = 0, 1; \tag{A1$a$}$$

and

$$Z_0(|k_2|\,r) = \begin{cases} -K_0(|k_2|\,r), & k_2^2 < 0, \\ \frac{1}{2}\pi Y_0(k_2 r), & k_2^2 > 0. \end{cases} \tag{A1$b$}$$

Further, conditions (3.6) rewritten in terms of the normal-mode variables (3.7) are imposed on the function $\bar{\psi}_{i,r}^{(0)}$. This entails the use of formulae (3.15*a*), (3.17*a*) and the well-known formulae for the derivatives of the Bessel functions, $G_n'$, $G_n''$ and $K_0'$, $K_n''$ (Abramowitz & Stegun 1965). As a result, the following system of linear equations in $A, D, B_0$, $B_0^{(\Lambda)}$ and $C_i$ is obtained:

$$\bar{\alpha}_i\left[\bar{A}\tilde{g}_i(a) + \frac{D}{k_i^2}\right] + C_i G_0(\bar{k}_i) = \varepsilon_{i,1} B_0 K_0(\bar{p}) + \varepsilon_{i,2} B_0^{(\Lambda)} K_0(\bar{p}_\Lambda), \tag{A2$a$}$$

$$-\bar{\alpha}_i \bar{A} a \tilde{g}_i'(a) + \operatorname{sgn}(k_i^2)\bar{k}_i C_i G_1(\bar{k}_i) = \varepsilon_{i,1} B_0 \bar{p} K_1(\bar{p}) + \varepsilon_{i,2} B_0^{(\Lambda)} \bar{p}_\Lambda K_1(\bar{p}_\Lambda), \tag{A2$b$}$$

$$-\bar{\alpha}_i \bar{A} a^2 \tilde{g}_i''(a) + k_i^2 a^2 C_i G_1'(\bar{k}_i) = \varepsilon_{i,1} B_0 \bar{p}^2 K_1'(\bar{p}) + \varepsilon_{i,2} B_0^{(\Lambda)} \bar{p}_\Lambda^2 K_1'(\bar{p}_\Lambda), \tag{A2$c$}$$

where an overbar designates differentiation. Equations (A2) determine the rider. In a similar way, using (3.6), (3.7), (3.15*c*) and (3.17*b*), we arrive at the system of linear equations in coefficients $A_i^{(1)}$, $B_1$ and $B_1^{(\Lambda)}$ that determine the antisymmetric component of the solution:

$$A_i^{(1)} G_1(\bar{k}_i) - \frac{\bar{\alpha}_i(k^2 U + \beta)}{k_i^2} a = \varepsilon_{i,1} B_1 K_1(\bar{p}) + \varepsilon_{i,2} B_1^{(\Lambda)} K_1(\bar{p}_\Lambda), \tag{A3$a$}$$

$$-\operatorname{sgn}(k_i^2) A_i^{(1)} \bar{k}_i^2 G_1(\bar{k}_i) = \varepsilon_{i,1} B_1 \bar{p}^2 K_1(\bar{p}) + \varepsilon_{i,2} B_1^{(\Lambda)} \bar{p}_\Lambda^2 K_1(\bar{p}_\Lambda), \tag{A3$b$}$$

$$\operatorname{sgn}(k_i^2) A_i^{(1)} \bar{k}_i G_2(\bar{k}_i) = \varepsilon_{i,1} B_1 \bar{p} K_2(\bar{p}) + \varepsilon_{i,2} B_1^{(\Lambda)} \bar{p}_\Lambda K_2(\bar{p}_\Lambda). \tag{A3$c$}$$

In (A2) and (A3), the notation is:

$$\bar{k}_i = |k_i|\,a,\ \bar{p} = pa, \quad \bar{p}_\Lambda = p_\Lambda a, \quad \varepsilon_{i,1} = 1 + \bar{\alpha}_i, \quad \varepsilon_{i,2} = \alpha_2 - \alpha_1\bar{\alpha}_i, \tag{A4$a$}$$

$$\bar{A} = \frac{\alpha_1 A}{2\pi}, \quad \tilde{g}_i = \frac{k^2 + p^2}{(k_i^2 + p^2)(k_i^2 + p_c^2)}\bar{g}_i. \tag{A4$c$}$$

The solvability condition for the system of equations (A3*b*, *c*) can be written as

$$\varepsilon_{1,1}\varepsilon_{2,2}(1 + H_1 Q)(1 + H_2 Q_\Lambda) = \varepsilon_{1,2}\varepsilon_{2,1}(1 + H_2 Q)(1 + H_1 Q_\Lambda), \tag{A5$a$}$$

where

$$H_1 = \frac{\bar{k}_1 I_1(\bar{k}_1)}{I_2(\bar{k}_1)}, \quad H_2 = \frac{\bar{k}_2 G_1(\bar{k}_2)}{G_2(\bar{k}_2)}, \quad Q = \frac{K_2(\bar{p})}{\bar{p} K_1(\bar{p})}, \quad Q_\Lambda = \frac{K_2(\bar{p}_\Lambda)}{\bar{p}_\Lambda K_1(\bar{p}_\Lambda)}. \tag{A5$b$–$e$}$$

Using (3.10), it will readily be seen that

$$\bar{\alpha}_1\bar{\alpha}_2 = -\frac{\Lambda_2}{\Lambda_1}, \quad \varepsilon_{1,1}\varepsilon_{2,2} = \frac{\alpha_2}{\bar{\alpha}_1}(1 + \bar{\alpha}_1)^2, \quad \varepsilon_{1,2}\varepsilon_{2,1} = \frac{\alpha_2}{\bar{\alpha}_2}(1 + \bar{\alpha}_2)^2. \tag{A6$a$–$c$}$$

Thus, the products $\varepsilon_{1,1}\varepsilon_{2,2}$ and $\varepsilon_{1,2}\varepsilon_{2,1}$ are opposite in sign. Because the parameters $H_1$, $Q$ and $Q_\Lambda$ are positive, condition (A5*a*) holds if $H_2$ is negative. This implies that $k_2^2 > 0$ and $G_n(\bar{k}_2) \equiv J_n(\bar{k}_2)$, $n = 0, 1, 2$ (compare (3.14*b*) and (3.16*a*)). Moreover, $H_2 < 0$ only if (3.19) is fulfilled.

It is a matter of direct verification to see that (A3*a*) and (A3*b*) are linearly dependent. Under condition (A5*a*), equations (A3*b*) and (A3*c*) are also linearly dependent. Thus, the resulting system of linearly independent equations consists of six equations: (A5*a*), equations

$$A_1^{(1)} I_1(\bar{k}_1) + \frac{\bar{\alpha}_i(k^2U+\beta)}{\bar{k}_1^2} a^3 = \varepsilon_{1,1} B_1 K_1(\bar{p}) + \varepsilon_{1,2} B_1^{(\Lambda)} K_1(\bar{p}_\Lambda), \tag{A7a}$$

$$A_1^{(1)} \bar{k}_1^2 I_1(\bar{k}_1) = \varepsilon_{1,1} B_1 \bar{p}^2 K_1(\bar{p}) + \varepsilon_{1,2} B_1^{(\Lambda)} \bar{p}_\Lambda^2 K_1(\bar{p}_\Lambda), \tag{A7b}$$

$$-A_1^{(1)} \bar{k}_1 I_2(\bar{k}_1) = \varepsilon_{1,1} B_1 \bar{p} K_2(\bar{p}) + \varepsilon_{1,2} B_1^{(\Lambda)} \bar{p}_\Lambda K_2(\bar{p}_\Lambda), \tag{A7c}$$

$$A_2^{(1)} \bar{k}_2 J_2(\bar{k}_2) = \varepsilon_{2,1} B_1 \bar{p} K_2(\bar{p}) + \varepsilon_{2,2} B_1^{(\Lambda)} \bar{p}_\Lambda K_2(\bar{p}_\Lambda), \tag{A7d}$$

and the equation that follows from (3.2*b*), (3.15*c*) and (3.16*a*):

$$\frac{1}{\bar{\alpha}_2 - \bar{\alpha}_1}\left[\frac{1}{2}\left(\bar{\alpha}_2 |k_1| A_1^{(1)} - \bar{\alpha}_1 k_2 A_2^{(1)}\right) + \bar{\alpha}_1\bar{\alpha}_2(k^2U+\beta)\left(\frac{1}{|k_1|^2} + \frac{1}{k_2^2}\right)\right] = -U. \tag{A7e}$$

To determine the antisymmetric component of the modon, we have seven equations: (A5*a*), (A7*a*)–(A7*e*), and (3.11) in eight unknowns, $A_1^{(1)}$, $A_2^{(1)}$, $B_1$, $B_1^{(\Lambda)}$, $k_1$, $k_2$, $U$ and $a$; the parameters $\bar{\alpha}_1, \bar{\alpha}_2$ and $k$ are expressed in terms of $k_1$, $k_2$ and $U$ using (3.9), (3.10). Thus, the family of solutions for the antisymmetric component is one-parameter. To solve these equations, the following algorithm is applied. Equations (A7*a*)–(A7*d*) are resolved with respect to $A_1^{(1)}$, $A_2^{(1)}$, $B_1$ and $B_1^{(\Lambda)}$; the coefficients $A_1^{(1)}$ and $A_2^{(1)}$ are then substituted into (A7*e*). The resulting equation and equations (3.11) and (A5a) constitute a nonlinear system of equations in $k_1, k_2, U$ and $a$. By fixing a specific translation speed $U$, we find $k_1$, $k_2$ and $a$, and, subsequently, calculate the coefficients $A_1^{(1)}$, $A_2^{(1)}$, $B_1$ and $B_1^{(\Lambda)}$.

Once the dipole component of the modon is known, the parameters of the rider can be calculated. Six parameters $\bar{A}$, $C_1$, $C_2$, $B_0$, $B_0^{(\Lambda)}$ and $D$ are determined by six equations (A2). These equations are linearly dependent and can be reduced to the following five equations in six unknowns:

$$\bar{\alpha}_1[-(k^2+p^2)\psi_{2,s}(a) + D] = \varepsilon_{1,1}\left(k_1^2+p^2\right) B_0 K_0(\bar{p}) + \varepsilon_{1,2}\left(k_1^2+p_\Lambda^2\right) B_0^{(\Lambda)} K_0(\bar{p}_\Lambda), \tag{A8a}$$

$$-\bar{\alpha}_i \bar{A} a \tilde{g}_i'(a) + \operatorname{sgn}(k_i^2)\bar{k}_i C_i G_1(\bar{k}_i) = \varepsilon_{i,1} B_0 \bar{p} K_1(\bar{p}) + \varepsilon_{i,2} B_0^{(\Lambda)} \bar{p}_\Lambda K_1(\bar{p}_\Lambda), \tag{A8b}$$

$$\begin{aligned} -\bar{\alpha}_i[k_i^2 a^2 \bar{A}\tilde{g}_i(a) + (k^2+p^2)a^2\psi_{2,s}(a)] - k_i^2 a^2 C_i G_0(\bar{k}_i) \\ = \varepsilon_{i,1} B_0 \bar{p}^2 K_0(\bar{p}) + \varepsilon_{i,2} B_0^{(\Lambda)} \bar{p}_\Lambda^2 K_0(\bar{p}_\Lambda). \end{aligned} \tag{A8c}$$

Given $\bar{A}$, the system of equations (A8) becomes well-defined and always has a non-trivial solution.

## Appendix B. Long-term asymptotic estimates

First, we consider the integrals in (4.14*c*), (4.14*d*) that determine the contribution of the baroclinic mode of the regular flow to the advection of the singular vortex. Our immediate aim is to show that

$$W_i \equiv \int_0^\infty r^2 K_1(r) \cos b_i t \, \mathrm{d}r = O\left(\frac{1}{t}\right), \quad t \to \infty. \tag{B1}$$

For this purpose, we apply integration by parts:

$$W_i = \frac{1}{t}\int_0^\infty \frac{r^2K_1(r)}{b_i'}d(\sin b_i t) = \frac{1}{t}\left[\frac{r^2K_1(r)}{b_i'}\sin b_i t\bigg|_0^\infty - \int_0^\infty \left(\frac{r^2K_1(r)}{b_i'}\right)'\sin b_i t\,\mathrm{d}r\right]. \tag{B2}$$

From (4.7), the following equations are obtained:

$$b_1' = -\frac{1}{r}\left(\alpha_1 p^2 K_2(pr) + \alpha_2 p_A^2 K_2(p_A r)\right), \quad b_2' = -\frac{\alpha_1}{r}\left(p^2 K_2(pr) - p_A^2 K_2(p_A r)\right), \tag{B3a, b}$$

yielding:

$$b_1' = -\frac{2}{r^3} + O\left(\frac{1}{r}\right), \quad b_2' = -\frac{\alpha_1}{2r} + O(r^2\ln r), \quad r\to 0, \tag{B4a, b}$$

$$b_i' = -\alpha_1\sqrt{\frac{\pi}{2}}p^{3/2}\frac{e^{-pr}}{\sqrt{r}}\left[1 + O\left(\frac{1}{r}\right)\right], \quad r\to\infty. \tag{B5}$$

By virtue of (B4), (B5),

$$\frac{r^2K_1(r)}{b_i'}\bigg|_0^\infty = 0, \quad \left(\frac{r^2K_1(r)}{b_i'}\right)'\bigg|_{r=0} = 0. \tag{B6a, b}$$

Lastly, because $p < 1$ (assumption (4.5)), the function $r^2K_1(r)/b_i'$ decreases exponentially with $r\to\infty$. Thus, both terms in square brackets in (B2) are bounded, which proves the estimate given by (B1).

Similarly, it can be shown that

$$\int_0^\infty r^2K_1(r)\sin b_i t\,\mathrm{d}r = O\left(\frac{1}{t}\right), \quad t\to\infty, \tag{B7}$$

Therefore, the contribution of the baroclinic $\beta$-gyres to the advection of the singular vortex goes to zero with time:

$$U_{BC} = O\left(\frac{1}{t}\right), \quad V_{BC} = O\left(\frac{1}{t}\right), \quad t\to\infty. \tag{B8}$$

Estimates (B1) and (B7) are also valid for the integrals in (4.11*c*), (4.11*d*). Therefore, at any fixed $r$,

$$\psi_{BC} = O\left(\frac{1}{t}\right), \quad t\to\infty. \tag{B9}$$

In other words, the baroclinic components of the $\beta$-gyres decrease with time.

The evolution of the barotropic mode is quite different: this component increases with time. To prove this statement, consider the following integrals:

$$P_c = \int_0^\infty r(1-\cos b_i t)\mathrm{d}r, \quad P_s = \int_0^\infty r\sin b_i t\,\mathrm{d}r. \tag{B10a, b}$$

The first of these integrals can be represented as

$$P_c = S_c + O(1), \quad S_c = \int_R^\infty r(1-\cos b_i t)\mathrm{d}r, \quad t\to\infty, \tag{B11}$$

where $R > 0$. Let $R$ be large enough to allow the substitution of the asymptotic expression

$$b_i = c\frac{e^{-pr}}{\sqrt{r}}\left[1 + O\left(\frac{1}{r}\right)\right], \quad c = \alpha_1\sqrt{\frac{\pi p}{2}} \tag{B12}$$

for $b_i$ in $S_c$ at large $r$. By changing the variable in the integral in (B11) from $r$ to $b_i$, we obtain:

$$S_c = -\int_0^B \frac{r(b_i)}{b_i'[r(b_i)]}(1 - \cos b_i t)\mathrm{d}b_i, \quad B = b_i(R). \tag{B13}$$

Resolving (B12) with respect to $r$ yields:

$$r = -\frac{1}{p}\ln b_i + O\left(\ln|\ln b_i|\right), \quad b_i' \cong -pb_i, \quad b_i \to 0, \tag{B14}$$

and substitution of (B14) into (B13) provides:

$$S_c \cong -\frac{1}{p^2}\int_0^B \frac{\ln b_i}{b_i}(1 - \cos b_i t)\mathrm{d}b_i. \tag{B15}$$

where the symbol $\cong$ is used to denote asymptotic equalities for $b_i \to 0$.

To estimate $S_c$ at large times, we introduce a new variable, $\bar{b}_i = b_i t$:

$$S_c \cong -\frac{1}{p^2}\int_0^B \frac{\ln b_i}{b_i}(1 - \cos b_i t)\mathrm{d}b_i = -\frac{1}{p^2}\left[\int_0^{Bt} \frac{\ln \bar{b}_i}{\bar{b}_i}(1 - \cos \bar{b}_i)\mathrm{d}\bar{b}_i - \ln t\int_0^{Bt} \frac{1 - \cos \bar{b}_i}{\bar{b}_i}\mathrm{d}\bar{b}_i\right]. \tag{B16}$$

It is easy to verify that

$$\int_0^{Bt} \frac{\ln \bar{b}_i}{\bar{b}_i}(1 - \cos \bar{b}_i)\mathrm{d}\bar{b}_i = \tfrac{1}{2}\ln^2 Bt + O(1), \tag{B17$a$}$$

$$\int_0^{Bt} \frac{1 - \cos \bar{b}_i}{\bar{b}_i}\mathrm{d}\bar{b}_i = \ln Bt + \gamma + O\left(\frac{1}{t}\right), \tag{B17$b$}$$

where $\gamma$ is a constant (e.g. Abramowitz & Stegun 1965). Substitution of estimates (B17) into (B16) leads to the asymptotic relationship

$$S_c = \frac{1}{p^2}\left(\frac{1}{2}\ln^2 t + \gamma\ln t + O(1)\right). \tag{B18}$$

Therefore,

$$P_c = \int_0^\infty r(1 - \cos b_i t)\mathrm{d}r = \frac{1}{p^2}\left(\frac{1}{2}\ln^2 t + \gamma\ln t\right) + O(1), \quad t \to \infty. \tag{B19}$$

In the same way, the asymptotic behaviour of $P_s$ is established. First, we can write:

$$P_s = S_s + O\left(\frac{1}{t}\right), \quad S_s = \int_R^\infty r\sin b_i t\,\mathrm{d}r, \quad t \to \infty, \tag{B20}$$

where $R > 0$. Next, $S_s$ is represented as

$$S_s = -\frac{1}{p^2}\int_0^B \frac{\ln b_i}{b_i}\sin b_i t\,\mathrm{d}b_i, \tag{B21}$$

yielding the equalities

$$S_s = -\frac{1}{p}\left[\int_0^{Bt} \frac{\ln \bar{b}_i}{\bar{b}_i} \sin \bar{b}_i \mathrm{d}\bar{b}_i - \ln t \int_0^{Bt} \frac{\sin \bar{b}_i}{\bar{b}_i} \mathrm{d}\bar{b}_i\right] = \frac{1}{p^2}\left[\frac{\pi}{2}\ln t - c_0 + O\left(\frac{\ln t}{t}\right)\right], \tag{B22a}$$

where

$$c_0 = \int_0^{\infty} \frac{\ln x}{x} \sin x \mathrm{d}x. \tag{B22b}$$

Lastly, relationships (B20), (B21) and (B22) provide:

$$P_s = \int_0^{\infty} r \sin b_i t \mathrm{d}r = \frac{1}{p^2}\left(\frac{\pi}{2}\ln t - c_0\right) + O\left(\frac{\ln t}{t}\right), \quad t \to \infty. \tag{B23}$$

Now the estimates given by formulae (B10*a*), (B10*b*), (B19) and (B23) are substituted into (4.14*a*), (4.14*b*). This yields:

$$U_{BT} = \frac{1}{p^2}\left[\frac{1}{2}\ln^2 t + \gamma \ln t\right] + O(1), \quad t \to \infty, \tag{B25a}$$

$$V_{BT} = \frac{1}{p^2}\left(\frac{\pi}{2}\ln t - c_0\right) + O\left(\frac{\ln t}{t}\right), \quad t \to \infty. \tag{B25b}$$

Thus, it can be concluded that the contribution of barotropic $\beta$-gyres to the advection of the singular vortex increases with time. Analogous asymptotic estimates of integrals in (4.11*a*), (4.11*b*) lead to the conclusion that, at a fixed $r$,

$$\psi_{BT} = r(-U_{BT} \sin\theta + V_{BT} \cos\theta) + O(1) \tag{B26}$$

with $t \to \infty$.

## REFERENCES


Abramowitz, M. & Stegun, I. A. 1965 *Handbook of Mathematical Functions*. Dover, New York.

Flierl, G. R. 1987 Isolated eddy models in geophysics. *Annu. Rev. Fluid Mech.* **19**, 493–530.

Flierl, G. R., Larichev, V. D., McWilliams, J. C. & Reznik, G. M. 1980 The dynamics of baroclinic and barotropic solitary eddies. *Dyn. Atmos. Oceans.* **5**, 1–41.

Flierl, G. R., Stern, M. E. & Whitehead, J. A. 1983 The physical significance of modons: laboratory experiments and general integral constraints. *Dyn. Atmos. Oceans.* **7**, 233–263.

Gryanik, V. M. 1986 The singular geostrophic vortices on the beta-plane as a model for synoptic vortices. *Oceanology* **26**, 126–130.

Gryanik, V. M. 1988 Localized vortices – 'vortex charges' and 'vortex filaments' in a baroclinic, differentially rotating fluid. *Izv. Atmos. Ocean. Phys.* **24**, 919–926.

Gryanik, V. M., Borth, H. & Olbers, D. 2004 The theory of quasi-geostrophic von Kármán vortex streets in the two-layer fluids on a beta-plane. *J. Fluid Mech.* **505**, 23–57.

Khvoles, R., Berson, D. & Kizner, Z. 2005 The structure and evolution of elliptical barotropic modons. *J. Fluid Mech.* **530**, 1–30.

Kizner, Z. I. 1984 Rossby solitons with axisymmetrical baroclinic modes. *Dokl. USSR Acad. Sci.* **275**, 1495–1498.

Kizner, Z. I. 1986*a* Intensity of synoptic eddies and the quasi-geostrophic approximation. *Oceanology* **26**, 28–35.

Kizner, Z. I. 1986*b* Strongly nonlinear solitary Rossby waves. *Oceanology* **26**, 382–388.

Kizner, Z. I. 1988 On the theory of intrathermocline eddies. *Dokl. USSR Acad. Sci.* **300**, 453–457.

Kizner, Z. I. 1997 Solitary Rossby waves with baroclinic modes. *J. Mar. Res.* **55**, 671–685.

Kizner, Z. 2006 Stability and transitions of hetonic quartets and baroclinic modons. *Phys. Fluids* **18**, 056601/12.

Kizner, Z. & Berson, D. 2000 Emergence of modons from collapsing vortex structures on the $\beta$-plane. *J. Mar. Res.* **58**, 375–403.

Kizner, Z., Berson, D. & Khvoles, R. 2002 Baroclinic modon equilibria on the beta-plane: stability and transitions. *J. Fluid Mech.* **468**, 239–270.

Kizner, Z., Berson, D. & Khvoles, R. 2003*a* Non-circular baroclinic modons: constructing stationary solutions. *J. Fluid Mech.* **489**, 199–228.

Kizner, Z., Berson, D., Reznik, G. & Sutyrin, G. 2003*b* The theory of the beta-plane baroclinic topographic modons. *Geophys Astrophys. Fluid. Dyn.* **97**, 175–211.

Larichev, V. D. & Reznik, G. M. 1976*a* On the two-dimensional solitary Rossby waves. *Dokl. Akad. Nauk SSSR* **231**, 1077–1079.

Larichev, V. D. & Reznik, G. M. 1976*b* Strongly nonlinear two-dimensional solitary Rossby waves. *Oceanology* **16**, 961–967.

McWilliams, J. C. & Flierl, G. R. 1979 On the evolution of isolated, nonlinear vortices. *J. Phys. Oceanogr.* **9**, 1155.

Mied, R. P. & Lindemann, G. J. 1982 The birth and evolution of eastward-propagating modons. *J. Phys. Oceanogr.* **12**, 213–230.

Nycander, J. 1988 New stationary vortex solutions of the Hasegawa – Mima equation. *J. Plasma Phys.* **39**, 418–428.

Reznik, G. M. 1986 Point vortices on a $\beta$-plane and Rossby solitary waves. *Oceanology* **26**, 165–173.

Reznik, G. M. 1987 On the structure and dynamics of a two-dimensional Rossby soliton. *Oceanology* **27**, 716–720.

Reznik, G. M. 1992 Dynamics of singular vortices on a $\beta$-plane. *J. Fluid Mech.* **240**, 405–432.

Reznik, G. M. & Dewar, W. 1994 An analytical theory of distributed axisymmetric barotropic vortices on the beta-plane. *J. Fluid Mech.* **269**, 301–321.

Reznik, G. & Kizner, Z. 2007 Two-layer quasi-geostrophic singular vortices embedded in a regular flow. Part 1. Invariants of motion and stability of vortex pairs *J. Fluid. Mech.* **584**, 185–202.

Reznik, G. M., Grimshaw, R. & Sriskandarajah, H. J. 1997 On basic mechanisms governing two-layer vortices on a beta-plane. *Geoph. Astrophys. Fluid. Dyn.* **86**, 1–42.

Reznik, G. M., Grimshaw, R. & Benilov, E. 2000 On the long-term evolution of an intense localized divergent vortex on the beta-plane. *J. Fluid. Mech.* **422**, 249–280.

Sutyrin, G. G. & Flierl, G. R. 1994 Intense vortex motion on the beta-plane: development of the beta-gyres. *J. Atmos Sci.* **51,** 773–790.

Sutyrin, G. G., Hesthaven, J. S., Lynov, J. P. & Rasmussen, J. 1994 Dynamical properties of vortical structures on the beta-plane. *J. Fluid Mech.* **268**, 103–131.

Tribbia, J. J. 1984 Modons in spherical geometry. *Geophys. Astrophys. Fluid Dyn.* **30**, 131–168.

Verkley, W. T. M. 1984 The construction of barotropic modons on a sphere. *J. Atmos. Sci.* **41**, 2492–2504.